

Landslides (2018) 15:475–488
 DOI 10.1007/s10346-017-0883-y
 Received: 15 February 2017
 Accepted: 22 August 2017
 Published online: 3 September 2017
 © Springer-Verlag GmbH Germany 2017

Fasheng Miao · Yiping Wu · Yuanhua Xie · Yaonan Li

Prediction of landslide displacement with step-like behavior based on multialgorithm optimization and a support vector regression model

Abstract Landslide prediction is important for mitigating geohazards but is very challenging. In landslide evolution, displacement depends on the local geological conditions and variations in the controlling factors. Such factors have led to the “step-like” deformation of landslides in the Three Gorges Reservoir area of China. Based on displacement monitoring data and the deformation characteristics of the Baishuihe Landslide, an additive time series model was established for landslide displacement prediction. In the model, cumulative displacement was divided into three parts: trend, periodic, and random terms. These terms reflect internal factors (geological environmental, gravity, etc.), external factors (rainfall, reservoir water level, etc.), and random factors (uncertainties). After statistically analyzing the displacement data, a cubic polynomial model was proposed to predict the trend term of displacement. Then, multiple algorithms were used to determine the optimal support vector regression (SVR) model and train and predict the periodic term. The results showed that the landslide displacement values predicted based on data time series and the genetic algorithm (GA-SVR) model are better than those based on grid search (GS-SVR) and particle swarm optimization (PSO-SVR) models. Finally, the random term was accurately predicted by GA-SVR. Therefore, the coupled model based on temporal data series and GA-SVR can be used to predict landslide displacement. Additionally, the GA-SVR model has broad application potential in the prediction of landslide displacement with “step-like” behavior.

Keywords Baishuihe Landslide · Displacement prediction · Time series · Three Gorges Reservoir · Support vector regression · Step-like displacement

Introduction

Landslides are one of the worst types of natural disasters, and they occur frequently around the world, particularly in mountainous regions (Hong et al. 2016a). Landslides are very typical in the Three Gorges Reservoir area of China (Du et al. 2013). The geological processes and conditions required for landslide formation are complex, making the collection of landslide evolution data an extremely difficult task. The landslide prediction field has developed rapidly and relied on incomplete kinematic monitoring data and unreliable landslide prediction theories. A reasonably accurate prediction could avoid human loss, reduce damages to property, and provide adequate countermeasures for design (Federico et al. 2012).

The prediction of landslide deformation started with the Saito model in the 1960s. Over the past 50 years, studies of landslide deformation prediction have yielded great achievements (Newcomen and Dick 2016). Currently, the prediction models based on deformation or displacement can be roughly classified into four types. The first type is empirical models, which are

mainly based on creep theory and use observed displacement monitoring data from landslides. These models generally describe the rheological functions of landslides, and the function variables include the displacement value or displacement speed. Representative empirical models include the Saito model (1965), Fukuzono model (1985), Hayashi model (1988), Voight model (1989), and other models (Crosta and Agliardi 2012; Mufundirwa et al. 2010). These models are derived from a wide range of actual observations and laboratory creep experiments and have a solid physical basis; therefore, they can be effectively applied for the prediction of landslides, volcano eruptions, earthquakes, and other disasters. However, the models have strict application conditions. The second type is statistical models, which are based on mathematical statistical methods and other prediction theories. These models include the gray system model (Deng 1988), Verhulst model (Yin and Yan 1996), plant growth model, and gray displacement vector angle model (Yang 1992). From displacement information, statistical trends can be obtained to determine the unknown displacement. These types of models can address landslide problems when the physical mechanisms of the landslide are too complicated to decode. Statistical models are most effective for addressing individual impact factors. However, the deformation of a landslide is affected by many factors that are not easily addressed using statistical models. The third type is nonlinear models, which are based on nonlinear theories, such as catastrophe theory (Qin 2005) and synergetic theory (Huang and Xu 1997). These models include the traditional nonlinear model (Liu et al. 2014; Yao et al. 2015), neural networks (Du et al. 2013; Lian et al. 2015), support vector regression (Pradhan 2013; Jebur et al. 2015; Zhou et al. 2016), the Newmark model (Chousianitis et al. 2014; Du and Wang 2016; Hwang and Chen 2013), and extreme learning machines (Cao et al. 2015). The fourth type is comprehensive models, which are combined with multifactor models to forecast landslide hazards. These models represent a new direction in temporal landslide prediction. For instance, autoregressive integrated moving average-based model is applied to landslide prediction (Carlà et al. 2016).

From the displacement monitoring curve (Fig. 1), landslides can be divided into four categories: steady-type landslide, which means the landslide displacement monitoring curve shows a steady growth trend. Exponential-type landslide: the landslide displacement monitoring curve shows an exponential growth trend, and the transition rate increases. Step-like landslide: due to the large increase and periodic fluctuation of the water level, the shape of the cumulative displacement-time curve of landslides in the special geological environment of the Three Gorges Reservoir shows the trend described as “step-like”. Convergent-type landslide: at first, the displacement speed of landslide is large and then gradually stabilized. Landslides with “step-like” deformation behavior experience several distinct acceleration phases followed by periods of relative stability before failure. The velocity of the

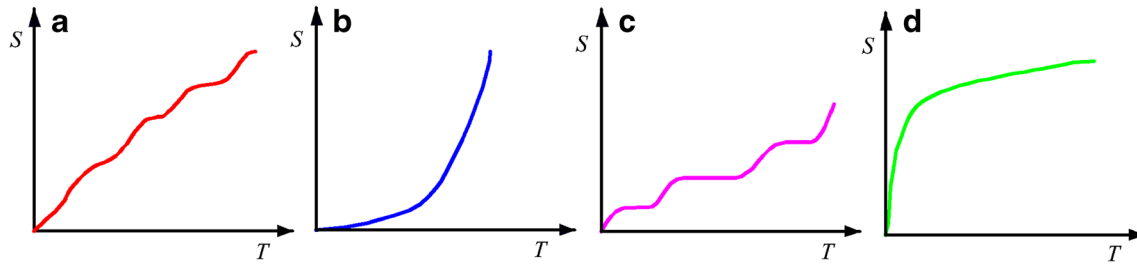


Fig. 1 Landslide classification based on the displacement monitoring curve. a Steady-type landslide. b Exponential-type landslide. c Step-like landslide. d Convergent-type landslide

displacement fluctuation combined with the rainfall quantity and water level in the reservoir are the major factors that contribute to these phases. The displacement curve consists of “power law” acceleration phases during external loading periods that are separated by phases of decreasing velocity during nonloading periods.

In this paper, considering the internal and external factors that affect landslide deformation and using the Baishuihe Landslide, which has a typical “step-like” behavior, as an example, the relationship between landslide development and the external influencing factors is investigated based on landslide deformation monitoring data. Through time series analysis, the accumulative displacement of a landslide is divided into three parts: trend terms, periodic terms, and random terms. Then, the displacement of each part can be predicted using a cubic polynomial and support vector regression based on multialgorithm optimization. The displacement prediction accuracy of each part can be analyzed quantitatively according to the goodness of fit (R^2) and mean square error (MSE) of the predicted values.

Methodology

Time series theory

The time series theory of nonstationary landslide displacement can be assumed by three parts (Yang 1992): a trend term that is controlled by the internal factors and geological conditions themselves, such as the geomorphology and geological structure; a periodic term that is affected by external factors, such as the reservoir water level and the rainfall intensity; and a random term that corresponds to random causal factors. Because multiple factors are involved in landslide deformation, the nonstationary time series theory is used to establish a dynamic model based on displacement observations and reflect the relationship between the evolution of landslide displacement and the impact factors. Therefore, the additive time series model can be generalized in the following form:

$$X(t) = \phi(t) + \eta(t) + \varepsilon(t) \quad (1)$$

where t is time, $X(t)$ is time series displacement, $\phi(t)$ is the trend term function, $\eta(t)$ is the periodic term function, and $\varepsilon(t)$ is the random term function.

Each function of the model corresponds with a part of landslide displacement theory; thus, the displacement prediction has clear physical and mathematical significance. In this study, the additive

time series model is used as the basic prediction model for the landslide with “step-like” behavior.

Support vector regression

The support vector regression (SVR) model was proposed by Vapnik (2000) and has been widely used in nonlinear problem solving (Bui et al. 2016a; Hong et al. 2015). In SVR models, sample data are divided into a training sample and test sample. Then, the input vector (training sample) chosen in advance is mapped to a high-dimensional feature space. Next, the best fitting effect is obtained in the space of the optimal decision function model, and the training sample is used to validate the analytical model results (Bui et al. 2016b; Hong et al. 2016b). The focus of this approach is forecasting analysis (Hong et al. 2016c; Bui et al. 2016c). A schematic diagram of SVR is presented in Fig. 2 (Zhou et al. 2016).

$\{x_j, y_j\}$ is a characteristic vector of sample data, where $x_j = \{x_{j1}, x_{j2}, \dots, x_{jp}\}$ is the impact factor of y_j and p is the number of values in y_j . The regression estimation function of the support vector machine (SVM) is as follows:

$$f(x) = W^T \phi(x) + b \quad (2)$$

where $\phi(x)$ is the nonlinear mapping function of the sample data, which are mapped to the feature space; W^T is the coefficient of the independent function; and b is the offset. W^T and b can be obtained by minimizing the following equation:

$$D(f) = \frac{1}{2} \|W\|^2 + \frac{C}{n} \sum_{j=1}^n R_\varepsilon [y_j, f(x_j)] \quad (3)$$

where $D(f)$ is the generalized optimal classification plane function, which considers the minimum number of incorrect sample points and the largest classification interval; $\|W\|^2$ is the complexity of the model; C is the penalty parameter; and R_ε is the insensitive loss (error control function) function of ε . Hence, the optimization problem can be expressed as follows:

$$\left. \begin{aligned} \min Q(W, \xi) &= \frac{1}{2} \|W\|^2 + C \sum_{j=1}^n \xi_j + \xi_j^* \\ W^T \phi(x_j) + b - y_j &\leq \varepsilon + \xi_j \\ y_j - W^T \phi(x_j) - b &\leq \varepsilon + \xi_j^* \\ \xi_j \geq 0, \xi_j^* &\geq 0 (j = 1, 2, \dots, n) \end{aligned} \right\} \quad (4)$$

where ξ_j, ξ_j^* are relaxation factors.

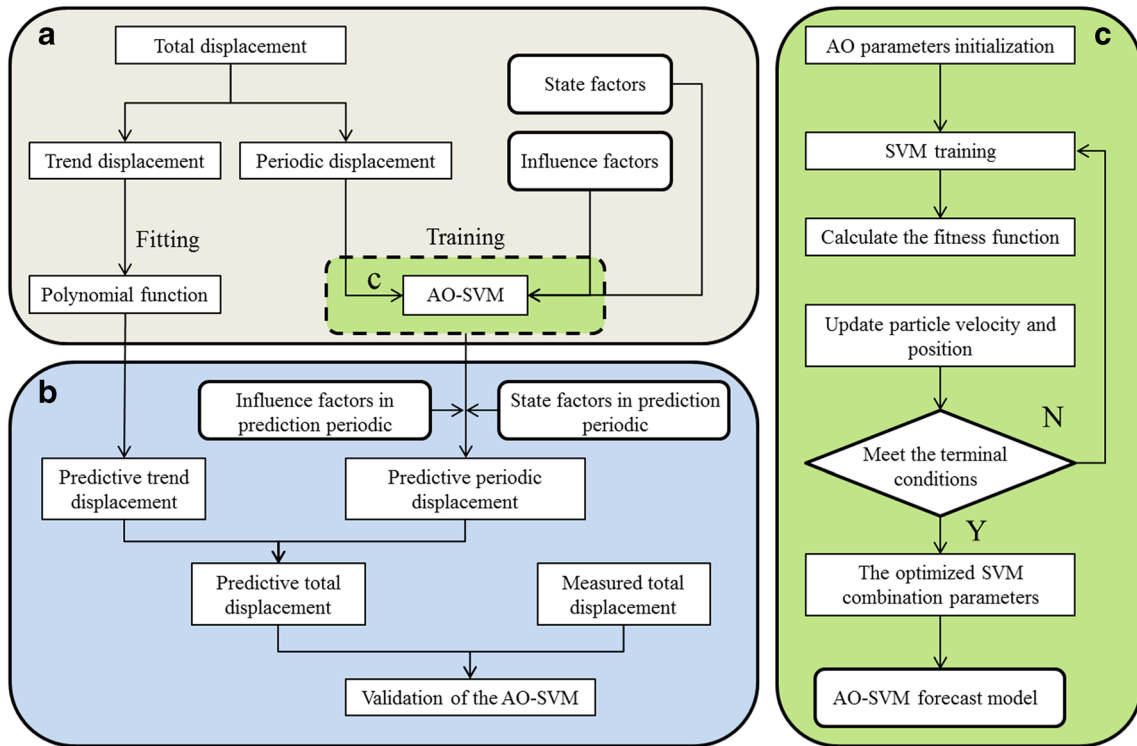


Fig. 2 Schematic diagram of algorithm optimization for SVR: (a) model creation, (b) model validation, and (c) AO-SVM model construction

Setting the partial derivatives of W , b , ξ_j , and ξ_j^* to 0 and using the Lagrange equation and duality theory, a dual optimization problem can be formed:

$$\left. \begin{aligned} L(W, a, b, \varepsilon, y) &= \min \frac{1}{2} \sum_{r,j=1}^n (a_r - a_r^*)^T H_{r,j} \\ a_r - a_r^* + \varepsilon \sum_{r,j=1}^n (a_r - a_r^*) + \sum_{r=1}^n y_r (a_r - a_r^*) \\ \sum_{r=1}^n (a_r - a_r^*) &= 0, (0 \leq a_r, a_r^* \leq C) \\ H_{r,j} &= K(x_r, x_j) = \phi(x_r)^T \phi(x_j), (r = 1, 2, \dots, n) \end{aligned} \right\} \quad (5)$$

where $K(x_r, x_j)$ is the kernel function, which is a polynomial function in this paper. The SVR model can then be established as follows.

$$f(x) = \sum_{j=1}^n (a_j^* - a_j) K(x_j, x) + b \quad (6)$$

The model, which is based on statistical learning theory, has numerous advantages. Notably, it requires a small sample size for learning, has a simple statistical structure, and performs better than traditional models of back propagation (BP) neural networks. Therefore, this model is advantageous for landslide displacement prediction.

The grid search algorithm

A grid search (GS) is a simple and straightforward method of finding the optimal parameter values for the SVM classifier.

Because the two parameters C and γ are independent, the GS process can be conducted in parallel. Specifically, a set of candidates is selected for both γ and C . Then, each pair of γ and C is evaluated by cross-validation, and the pair with the highest accuracy is considered the optimal solution (Gao and Hou 2016). The process involves a search within a certain range of the grid space in accordance with the relevant values of parameters in each step. Then, all points within the grid space are iteratively considered, and the performance of each parameter set is evaluated. Finally, the optimal parameter set that yields the optimal performance is selected. The disadvantage of the method is that when the range of the grid space is large and the step size is small, a long processing time is required.

The genetic algorithm

The genetic algorithm (GA) was inspired by the hypothetical mechanism of natural selection, in which the fittest individuals in a generation are more likely to survive and produce the next generation. GA is used to search for optimal solutions when the evaluation of all possible solutions is too costly in terms of the computational time (Taskin K et al. 2015). GA method is very robust, and implicit parallelism and global search capabilities are two important features of GAs. In a GA, each feasible solution is first encoded. Then, the solution space is transformed into a chromosome space, and the fitness of each chromosome is defined. Specifically, the fitness values of “preferred” individuals are higher than those of other individuals, i.e., individuals with large fitness values are more fit. Based on genetic operators such as selection, crossover, and mutation in a population, the group constantly evolves in the direction of the optimal solution. The

two-parameter GA and the three-parameter GA (cpg) are commonly used.

Particle swarm optimization

The particle swarm optimization (PSO) algorithm is a global optimization algorithm that was proposed by Eberhart and Kennedy (1995). In PSO, every particle is regarded as a solution to the optimization problem, and each particle acquires “flying experience” based on its experiences and those of other particles. A fitness function is defined to determine the superiority of each particle and search for the optimal solution in the entire solution space. The search principle is that each particle in the solution space approximates two points at the same time. The first point represents the best value obtained by any particle in the population in the process of searching for the global optimal solution q_{best} . The other point represents the optimal solution p_{best} achieved during the search process. Then, through iterations, the position and speed of the particle can be updated.

Case study: Baishuihe Landslide

Geological conditions

The Baishuihe Landslide is located on the right bank of the Yangtze River, 56 km from the Three Gorges Dam site (Fig. 3). As a large thick layer of sloping soil, the main sliding direction of the landslide is 20° with respect to N. The landslide has a 500-m length from north to south, a 430-m width from east to west, and an approximately 30-m average thickness. The volume of the landslide is $645 \times 10^4 \text{ m}^3$, covering an area of $21.5 \times 10^4 \text{ m}^2$. The rear

elevation is 450 to 500 m, and the front elevation is 120 to 130 m (Fig. 4). The Baishuihe Landslide formed in a nearly north-south gully with the south higher than the north, and it spread into the Yangtze River. The gradients of the leading edge and trailing edge of the landslide are large, and the central portion is flat. The morphology of the area shows irregular concave terrain on both sides of the landslide, and these areas are slightly higher than the middle of the landslide. Because the Baishuihe Landslide has been in an unstable state for several years, landslide warnings have been issued many times, especially since intense deformation occurred during the flood season in 2003. By the end of July 2012, the cumulative maximum displacement of the Baishuihe Landslide reached 3108.5 mm. Additionally, the deformation of cross-section 2–2' has considerably increased (Fig. 5).

The materials of the landslide are quaternary deposits, including silty clay and fragmented rubble with a loose and disorderly structure. The lithologies of the bedrock and strata that outcrop around the landslide are mainly Jurassic siltstone, arenaceous shale, and quartz sandstone, with dip directions of 15° and dip angles of 36° (Fig. 5).

Based on surface displacement monitoring, the Baishuihe Landslide can be divided into 2 major areas. The first area is the warning zone (sector A), which is the front part of the landslide that has undergone serious deformation. Because of the increase in reservoir storage when the Three Gorges Dam was built, the landslide has experienced obvious displacement, and multiple transverse tension cracks can be observed in the eastern part of the landslide (Fig. 4). Notably, large cracks have formed on the east side and rear boundary of the landslide, and weathering cracks

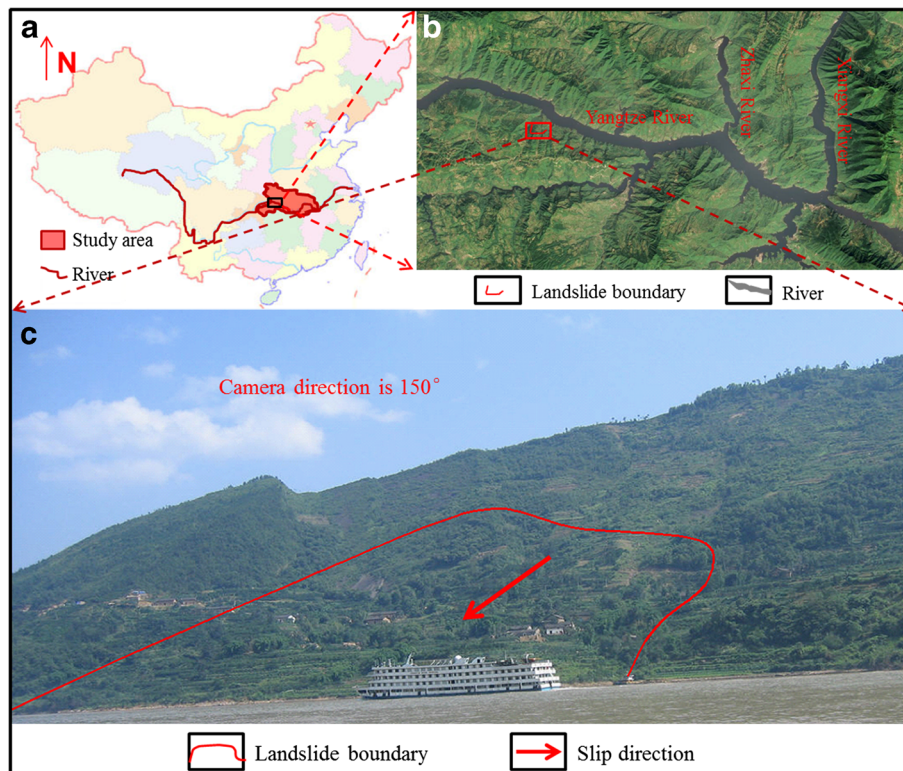


Fig. 3 a Location of the study area. b Location of the Baishuihe Landslide. c Geomorphology of the Baishuihe Landslide.

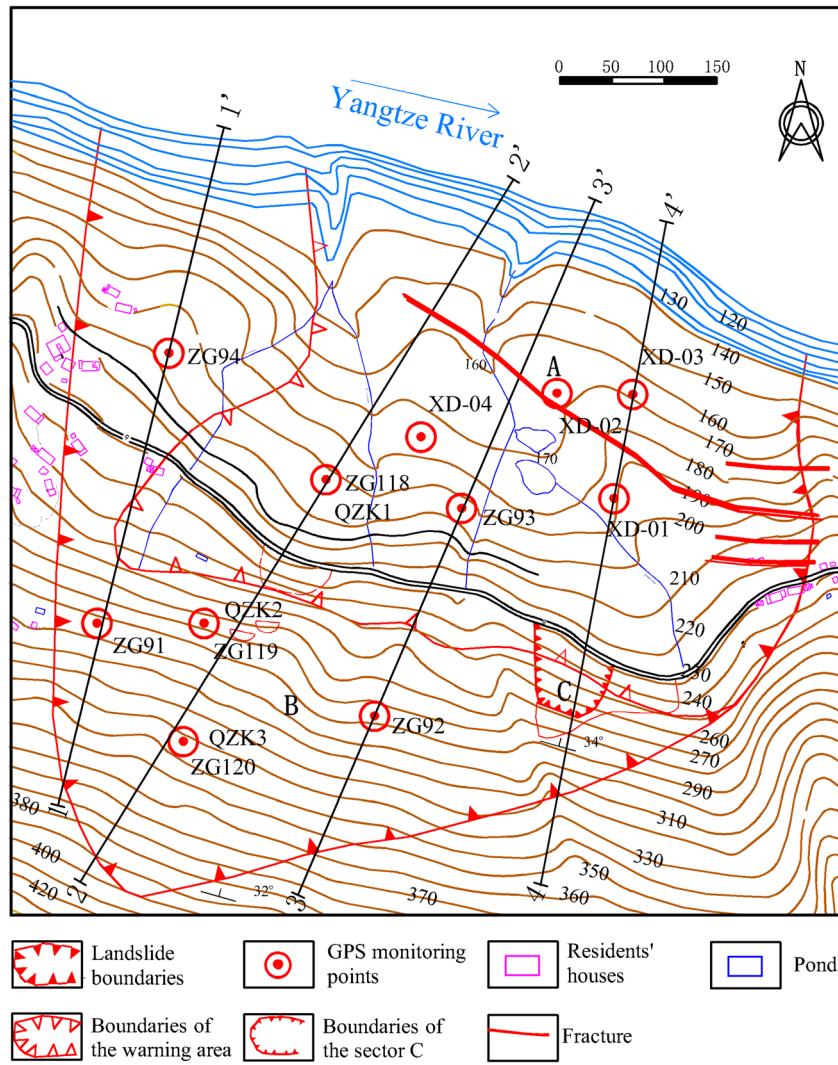


Fig. 4 Topographical map of the Baishuihe Landslide with the location of the monitoring network

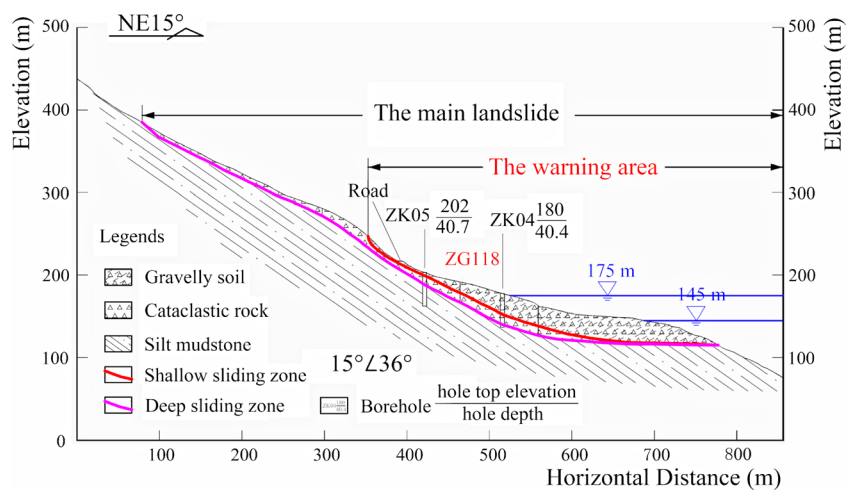


Fig. 5 Schematic geological cross-section (2-2') of the Baishuihe Landslide

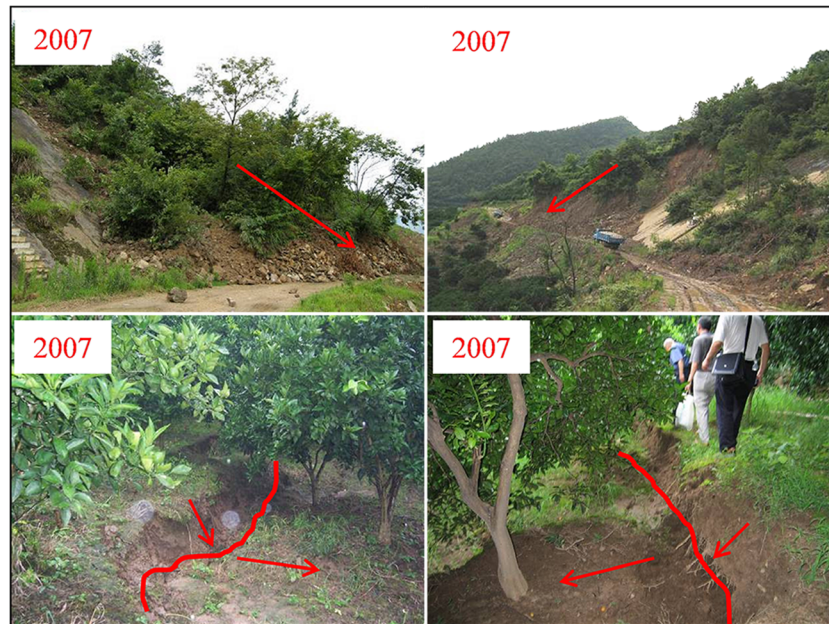


Fig. 6 Macroscopic deformation of the Baishuihe Landslide

have formed on the western boundary. On the morning of June 30, 2007, approximately 100,000 m³ of a highway landslide piled on the road in the posterior of the warning area, which is sector C (Fig. 4). The second area is relatively stable (sector B) and located at the back of the landslide. Cumulative deformation is small in this area, and the rate of deformation is slow at only 1.5 ~ 4.0 mm/year.

Deformation mode of the landslide

The Baishuihe Landslide is an old landslide that frequently reactivates. Landslide deformation monitoring began after obvious deformation was observed due to the initial impoundment of Three Gorges Reservoir in June 2003. Surface displacement monitoring was performed using a global positioning system (GPS). And the lateral displacement was monitored by inclinometer. The monitoring points are shown in Fig. 4. A total of seven GPS and three inclinometer deformation monitoring points were initially established on the surface of the landslide. In addition, four GPS deformation monitoring points were added in May 2004 and October 2005.

According to a report (Three Gorges University 2013), several landslides occurred at an elevation of approximately 220 m between August 2005 and August 2006. These landslides were small, generally on the order of tens of cubic meters. Additionally, sinking cracks appeared over a large area of the landslide surface. On the morning of June 30, 2007, the trailing edge of the warning area boundary was mainly connected. After August 2009, landslide displacement continued in a “step-like” process, and the western boundary cracks spread as intermittent plumes. The macroscopic deformation of the Baishuihe Landslide is shown in Fig. 6.

Evolution mode of the landslide

The Baishuihe Landslide is a typical retrogressive landslide; thus, the failure began at the bottom of the slope (Fig. 7). The sliding

surface is an approximately straight line, and the upper part of the landslide has a relatively steep slope and shallow depth. Deformation has mainly occurred in areas below 250 m of elevation. The displacement rates at the monitoring points in the front part of the landslide (XD-02, XD-03, and XD-04) were much higher than those at monitoring points ZG93 and ZG118 (Du et al. 2013).

The short-term deformation of the landslide with step-like behavior in the Three Gorges Reservoir area is triggered by the periodic fluctuation of the reservoir level and rainfall, as discussed in the next section. However, the influence of these triggers on the deformation is closely related to the evolutionary state of the landslide. Under the influence of the same triggers, landslides in various states deform differently. Therefore, it is difficult to accurately forecast landslide deformation by considering only the triggers and ignoring the evolutionary state of the landslide (Zhou et al. 2016). The progress of the landslide from beginning deformation to global sliding failure generally includes the primary creep, secondary creep, and the tertiary creep (Fig. 8). The

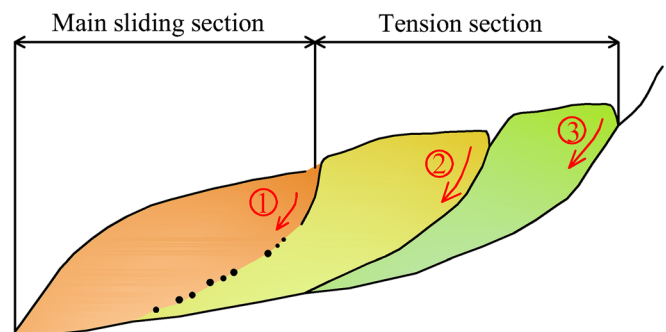


Fig. 7 Sketch of the deformation mechanism of the retrogressive Baishuihe Landslide

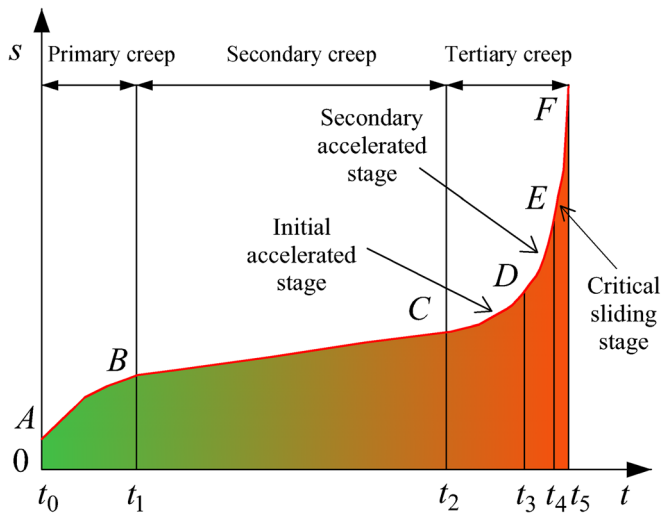


Fig. 8 Illustration of the three phases of slope deformation

displacement of the Baishuihe Landslide reflects a step-like change in the cumulative displacement curve from May to December of every year since 2003, corresponding to rainfall in the annual flood season. Therefore, rainfall in the flood season is the main factor that contributes to the steps in the landslide monitoring curves. However, in 2007, the landslide was not only influenced by rainfall in the flood season but also by the change in the normal water level of Three Gorges Reservoir at the same time. Thus, the cumulative displacement increase in June 2007 was one of the largest deformations due to the joint actions of rainfall and water level scheduling (Fig. 9). Landslide failure did not occur after the major deformation in 2007. Thereafter, a step-like change still existed in the annual cumulative displacement curves from May to October, and the range of the step decreased each year. Therefore, by observing the displacement over a multiyear period, it can be inferred that the landslide remained in a constant creep stage at the end of 2011.

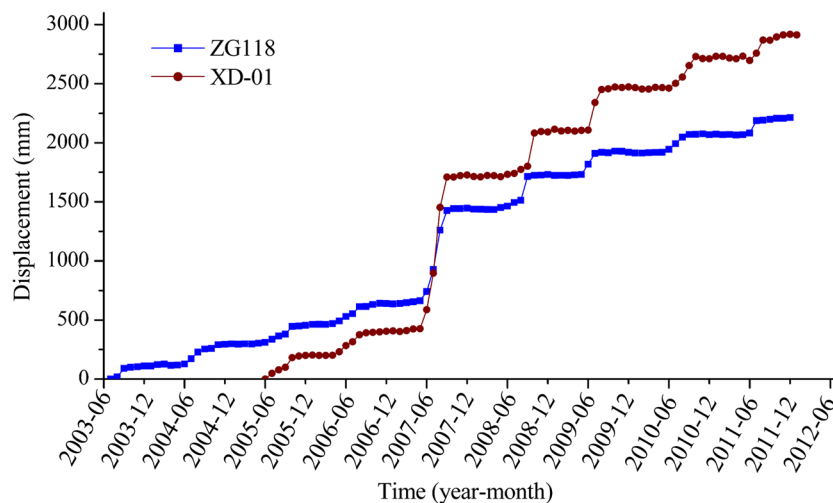


Fig. 9 Displacement monitoring curve of the Baishuihe Landslide

Analysis of the monitoring data

Inclinometer QZK1 (ZG118) indicated that the main sliding zone was located at a depth varying from 12 to 21.5 m (Fig. 10). The deep sliding zone was located 0.6 to 1 m above the siltstone bedrock.

Due to differences in the displacement monitoring periods, the monitoring cycles of ZG118 and XD-01 are longer than those of other stations. Therefore, this paper selects both sites for detailed analysis.

The rainfall, reservoir water level, and displacement data from the Baishuihe Landslide area from January 2008 to December 2011 (Three Gorges University 2013) are shown in Fig. 11. The main characteristics of the monitoring data are as follows:

- (1) Different monitoring points on the Baishuihe Landslide exhibit similar rates of displacement. Additionally, the landslide has the tendency to undergo intact slip. The landslide velocity is generally highest from May to August, which is the end of the period of decreasing water level. From September to April of the following year, the landslide displacement remains stable, which suggests that the change in landslide displacement is highly correlated with the reservoir water level, in this case, the increase in water level. In addition, landslide displacement exhibits a “lag effect”. Notably, the water level began to decline 1~2 months before landslide displacement began to gradually increase, and when the water level stopped decreasing, landslide displacement continued for 1~2 months.
- (2) Rainfall in Zigui County is concentrated from May to October. The results show that monthly displacement exhibits good agreement with variations in the monthly rainfall intensity. Additionally, the shape of the monthly rainfall curve is generally coincident with that of monthly displacement.

In conclusion, when the reservoir stores water, the slope floods and the groundwater level of the landslide gradually increases; however, the slope is affected by hydrostatic pressure from the water, and the force is orthogonal to the slope surface and in the

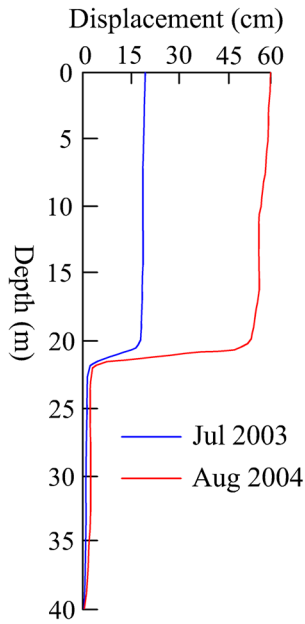


Fig. 10 Lateral displacement versus depth from inclinometer ZG118 (ZG118)

direction of the slope. Thus, this force increases the slope stability of the landslide. When the water level drops, a hydraulic gradient is formed because the groundwater level below the slope decreases more slowly than the water level in the reservoir. When the groundwater level and the reservoir level are equal, the hydraulic gradient disappears, and a pressure force forms that is not orthogonal to the slope. Therefore, the stability of the slope decreases. Additionally, rainfall forms surface runoff, which causes erosion on the slope surface, and infiltration that reaches the groundwater table increases the weight of the slope and softens the rock mass. These processes are not conducive to the stability of the slope. Hence, the reservoir level and rainfall are the most important factors that affect landslide displacement.

Calculations and results

In this paper, the cumulative displacement series of the Baishuihe Landslide from January 2008 to December 2011 is adopted as the

original time series. The cumulative displacement series from January 2008 to June 2011 is considered the training sample, and the cumulative displacement series from July 2011 to December 2011 is the test sample.

Trend term prediction

The trend term represents the main mode of the development of landslide deformation. Considering the characteristics of the cumulative displacement curves, the displacement in the flood season exhibit “step-like” growth over an annual period. Therefore, the moving average method was used to smooth the displacement curve, and the moving average is regarded as the trend term of landslide displacement. This method can reflect the abrupt changes in the displacement curves caused by the cyclical reservoir water level fluctuations and rainfall. The original displacement time series can be expressed as follows: $X_i = \{x_1, x_2, x_3, \dots, x_t\}$.

Based on this expression, the trend term of displacement can be written in the following form:

$$\varepsilon(i) = \frac{x_i + x_{i-1} + \dots + x_{i-n+1}}{n}, \quad (i = n, n + 1, n + 2, \dots, t) \quad (8)$$

where the n is the periodic value. In this paper, we set $n = 12$. Based on the cumulative displacement curves, the extracted trend term is shown in Fig. 12.

The model of trend term prediction can be constructed based on the shape of the growth curve of displacement. The least squares method was used to fit the curve when it was in linear or power function form, and the GM (1, 1) model was used to describe the curve when in exponential function form.

The GM (1, 1) model and Verhulst growth model were used to fit the trend term of displacement. However, the accuracies of these methods were low in this case. Because these two models are not applicable to the Baishuihe Landslide, the least squares method of polynomial fitting was adopted, and a cubic polynomial form was used.

$$\varepsilon(t) = at^3 + bt^2 + ct + d \quad (9)$$

The calculation results are shown in Table 1.

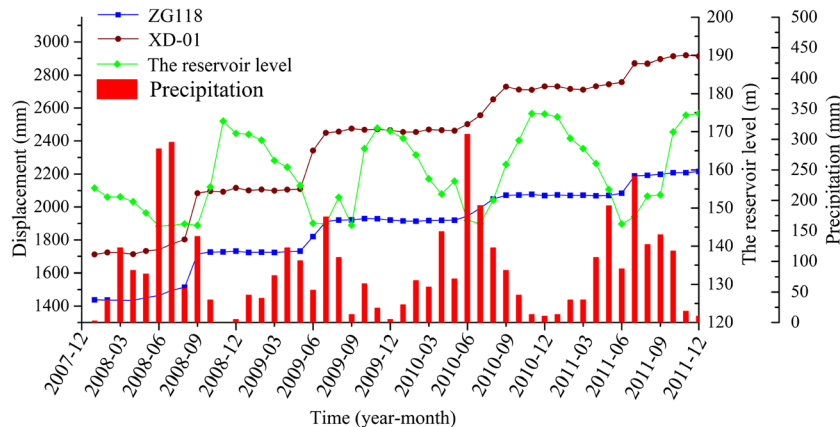


Fig. 11 Rainfall, reservoir water level, and cumulative displacement monitoring data from the landslide area

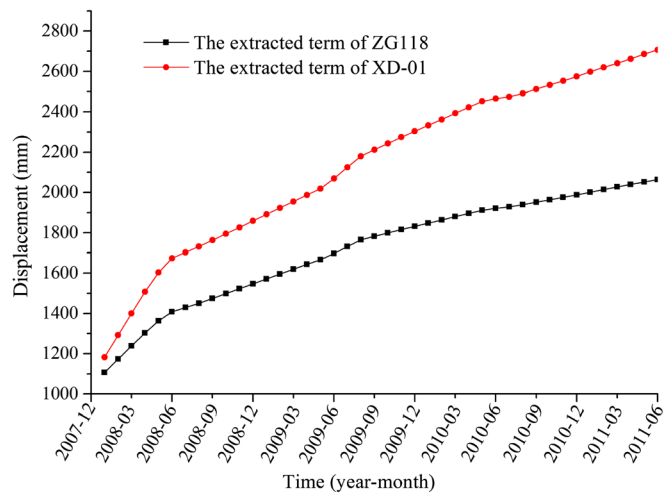


Fig. 12 Extracted trend term of displacement over time

The parameters of polynomial fitting (Table 1) were used to predict the trend term, and the results are shown in Fig. 13. Overall, the results of trend term prediction are good, mainly because the moving average method can eliminate the influence of the “step” in the cumulative displacement curve.

Periodic term prediction

Periodic term extraction

According to the additive time series model, cumulative displacement includes a periodic term and random term after removing the trend term. The extraction results of detrended displacement are shown in Fig. 14a. The fluctuations in the detrended displacement at the two monitoring points show that the displacement fluctuates periodically with changes in the reservoir water level and rainfall.

Factors that influence periodic displacement

The selection of the factors that influence displacement will directly affect the training capacity of the model. As noted above in the analysis of landslide monitoring data, the periodic displacement of the landslide is controlled by rainfall and the reservoir water level.

Precipitation Rainfall is one of the major external forces that trigger landslides in the Three Gorges Reservoir area (Tomas et al. 2014). Landslides are liable to occur in areas with continuous and torrential rainfall (Bernardie et al. 2015; Bordoni et al. 2015; Segoni et al. 2015). Additionally, rainfall infiltration can cause soil water changes, such as increasing the hydrodynamic and

hydrostatic pressures due to seepage. These processes can destabilize slopes by decreasing stabilizing forces and matrix suction. Moreover, rainfall infiltration causes chemical reactions in the soil. For example, rainfall infiltration can reduce the cohesive force and internal friction angle of a slope as a result of argillization and soil softening, disintegration, and dissolution due to reactions between soluble and hydrophilic minerals and infiltrated rainwater (Liu et al. 2003). Previous research on the relationship between landslides and rainfall suggests that precipitation 1 or 2 months before failure strongly promotes landslide deformation (Du et al. 2013). Because rainfall infiltration is a relatively slow process, the cumulative antecedent precipitation in the past 1 month and over the past 2 months was adopted as the rainfall factor to predict the periodic displacement of the landslide (Fig. 14)b.

The reservoir level Periodic fluctuations in the reservoir water level can lead to the step-like deformation of landslides in the Three Gorges Reservoir area (Jiao et al. 2014). Because water level fluctuations affect the distribution of the hydrodynamic field, the shear strength of the rock and soil slope decreases, the permeability changes, and the hydrostatic or dynamic pressure changes, causing slope instability (Li et al. 2004). Moreover, the effect of the reservoir level varies with the size of the fluctuation. Additionally, the influence of a fluctuation on landslide deformation varies based on the initial reservoir level. Considering the “delay effect” of the water level, 1- and 2-month base-level changes were adopted to represent the influence of reservoir scheduling on the deformation of the Baishuihe Landslide (Fig. 14)c.

Cumulative displacement increment per year: because of periodic variations in the reservoir water level and rainfall, the cumulative

Table 1 The parameters of the trend term of displacement based on polynomial fitting

Point	Parameters <i>a</i>	<i>b</i>	<i>c</i>	<i>d</i>	Accuracy (R^2)
ZG118	0.0089	-0.9901	48.73	1103.6	0.996
XD-01	0.0114	-1.2771	69.17	1211.9	0.9929

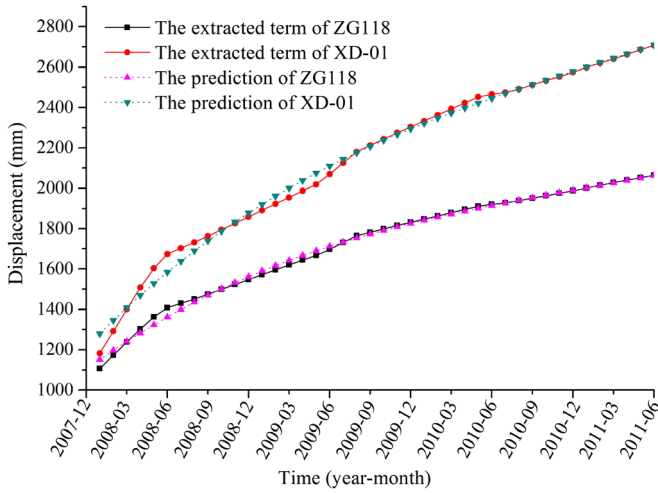


Fig. 13 Prediction and comparison of the trend term of displacement

displacement curve of the landslide exhibits periodic steps. Therefore, the annual rate of landslide displacement is inherently periodic (Fig. 14) d.

Using the gray correlation analysis method (Deng, 1988), a resolution coefficient of 0.5 was obtained, and the relational degree r_k between the impact factors and the periodic displacement is shown in Table 2. The impact factors are

closely related to the periodic displacement, as $r_k > 0.6$, suggesting that the parameters were properly selected (Wang et al. 2004).

Parameter setting in the models

GS-SVR model parameter setting In sample data preprocessing, all the factors and the periodic term of displacement must be converted to $[-1, 1]$ format. In GS parameter setting, the penalty factor $c = [0, 100]$, the kernel function parameter $g = [0, 100]$, the principal component is set to 95%, the grid range of c is $[-8, 8]$ and the grid step is 0.5, and the grid range of g is $[-8, 8]$ and the step is 0.5.

GA-SVR model parameter setting In sample data preprocessing, all the factors and the periodic term of displacement are converted to $[-1, 1]$ format. In GS parameter setting, the penalty factor is $c = [0, 100]$, the kernel function parameter is $g = [0, 100]$, the principal component is set to 95%, and the cross-validation value is $\nu = 5$.

PSO-SVR model parameter setting In sample data preprocessing, all the factors and the periodic term of displacement are converted to $[-1, 1]$ format. In GS parameter setting, the penalty factor is $c = [0, 100]$, the kernel function parameter is $g = [0, 100]$, the principal component is set to 95%, and the cross-validation value is $\nu = 5$. The population of the particle swarm is 20, the maximum number of evolutionary iterations is 100, and the inertia weight $isw = 1$.

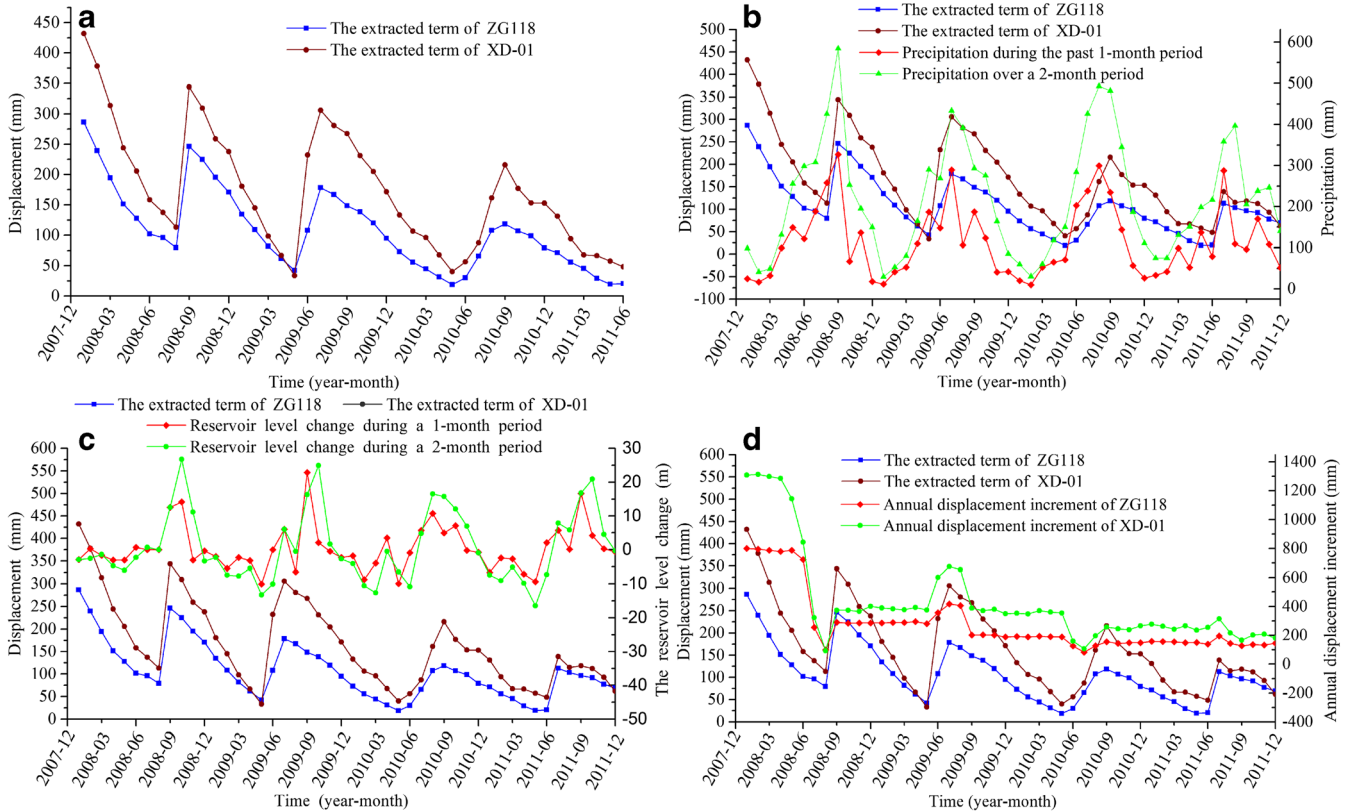


Fig. 14 a Detrended displacement. b Relationship between rainfall and periodic displacement. c Relationship between reservoir level change and periodic displacement. d Relationship between annual displacement and periodic displacement

Table 2 Relational degree between impact factors and periodic displacement

Point	Impact factors 1-month precipitation	2-month precipitation	Reservoir level	1-month level change	2-month level change	Annual displacement rate
ZG118	0.779	0.779	0.827	0.838	0.826	0.794
XD-01	0.791	0.790	0.826	0.840	0.824	0.751

Table 3 Optimal parameters of SVR used for the dataset

Point	GS-SVM		GA-SVM		PSO-SVM		GA(cpg)-SVM		P
	C	g	C	g	C	g	C	g	
ZG118	45.25	0.125	3.15	26.62	28.74	0.462	58.47	0.41	0.13
XD-01	8.00	0.01	1.27	35.43	5.80	0.01	38.86	0.32	0.18

GA(cpg)-SVR model parameter setting In sample data preprocessing, all the factors and the periodic term of displacement are converted to $[-1, 1]$ format. In GS parameter setting, the penalty factor is $c = [0, 100]$, the kernel function parameter is $g = [0, 100]$, $p = [0, 1]$, and the principal component is set to 95%.

Forecasting comparison of each model

Using the GS, GA, PSO, and GA (cpg) algorithms to search for the optimal penalty factor c , the kernel function parameter g is shown in Table 3. The training sample was assessed using the parameters obtained, and the model of periodic displacement prediction was constructed. The prediction accuracy and error of each model are shown in Table 4. Periodic displacement prediction and a comparison of results are shown in Fig. 15.

When predicting the periodic term of ZG118, the R^2 of each model and the root mean square error (RMSE) reflect similar trends. When predicting the periodic term of XD-01, the R^2 values of GA-SVR and GA (cpg)-SVR are much larger than those of GS-SVR and PSO-SVR. In October 2008, the predicted periodic displacement exhibited large fluctuations, especially at the XD-01 monitoring points, likely because October is the end of the peak rainfall period, and the heavy rain influences the slope displacement with a certain “lag effect.”

The comparison of the performance of the displacement prediction models shows that the GA-SVR model performs better than the GS-SVR and PSO-SVM models. Therefore, when performing random displacement prediction, the GA-SVR model is preferred.

Table 4 Prediction accuracy and error of each model

Model	R^2		RMSE	
	ZG118	XD-01	ZG118	XD-01
GS-SVR	0.940	0.755	16.556	53.461
GA-SVR	0.984	0.982	12.322	19.247
PSO-SVR	0.970	0.760	11.815	54.043
GA(cpg)-SVR	0.971	0.963	11.298	19.073

Random term prediction

After removing the trend term and the periodic term from the cumulative displacement series, the remaining part is the random term. The results are shown in Fig. 16.

The random term is trained by the displacement prediction model based on GA-SVM. In sample data preprocessing, all impact factors and periodic term displacements are converted to $[-1, 1]$ format. The GA algorithm parameters are set as follows: the punishment factor is $c = [0, 100]$, the kernel function parameter is $g = [0, 100]$, the principal component is 95%, and the cross-validation value is $\nu = 5$. The optimal parameters and accuracy of the model are shown in Table 5. Random term prediction is shown in Fig. 17.

Cumulative displacement prediction

Similarly, using the additive time series model, the cumulative displacement at ZG118 and XD-01 from January 2008 to December 2011 can be determined. The relationship between the observed and predicted displacement is shown in Fig. 18.

According to Fig. 18, in the early stage of sample training, both the absolute and relative errors at each point are much larger than the average values. As the number of training samples increases, the training effect improves. Additionally, as the number of prediction test samples increases, the absolute and relative errors increase. Therefore, the method proposed in this study exhibits high precision in the short-term prediction of landslide with step-like behavior displacement. However, the prediction accuracy decreases as the number of prediction test samples increases.

The comparison of the observed and predicted displacements at these two monitoring points shows that the curve of the predicted displacement corresponds well to the curve of the observed displacement. The predicted values fit the initial sample data and can predict displacement 6 months into the future. The model reflects the increasing trend in cumulative displacement, and the model is adequate for the displacement prediction of the Baishuihe Landslide.

Discussion

The deformation of the landslide with step-like behavior in the Three Gorges Reservoir area is triggered by the periodic factors,

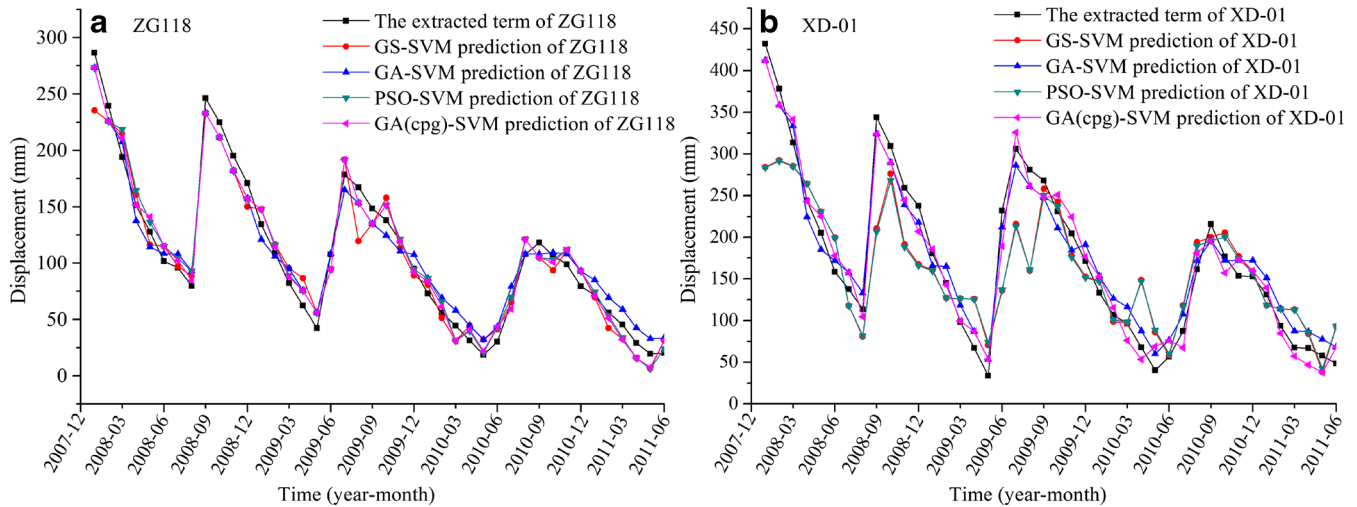


Fig. 15 Prediction and comparison of periodic displacement

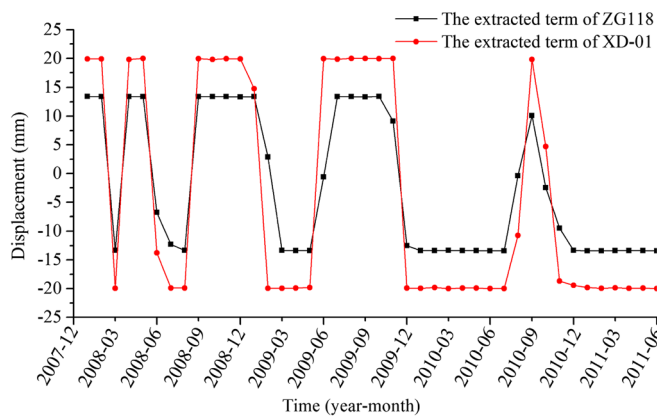


Fig. 16 Extraction of the random term of displacement with time

such as fluctuation of the reservoir level and the rainfall. But the influence of the factor triggers on the deformation development of landslide is closely related to its evolution state. Therefore, it is inaccurate to predict the deformation of landslide accurately by only considering the triggers and ignoring the evolution state of the landslide (Zhou et al. 2016). It can be inferred that the landslide remained in a constant creep stage from 2008 to 2011. Considering the primary creep state before 2007, the displacement data before 2007 is not adopted to be trained. In the paper, landslide displacement with step-like behavior is predicted based on multialgorithm optimization and SVM. And then, the results can be used for other research. Predicted displacement of Baishuihe Landslide is used to compute the alert velocity thresholds. Pre-alert, alert and

emergency velocity thresholds of each monitoring point are obtained respectively (Li et al. 2010). Crosta and Agliardi (2003) point out that surface displacement measurements can be used for failure forecast. Carlà et al. (2017) propose that displacements could be provided to establish ultimate alarm thresholds of impending slope failure risk at mine operations.

Random term of the landslide displacement is caused by random factors such as the wind load and vehicle load. Current detection methods are not suitable for accurately monitoring these random factors. Therefore, it is difficult to obtain the associated data, and these factors are generally not considered in studies. Before building a random SVM model in this paper, we attempted to treat the random term as a stationary time series and built an M-order autoregressive model to predict it. However, the results were not optimal. Therefore, GA-SVR model is chosen to fit this term. Notably, the accuracy at the two monitoring points reaches 0.771 and 0.741. Although there is a certain gap in accuracy between the random term and the periodic term, the trend of the random term can be reflected to a certain extent. In this paper, the trend term is predicted using a cubic polynomial model, and the accuracy reaches 0.996 and 0.9929 at the two monitoring points. The periodic term and the random term are predicted by GA-SVR, and the accuracy reaches (0.984, 0.982) and (0.771, 0.741), respectively, at the two points. Additionally, the overall accuracy of the prediction of Baishuihe Landslide displacement reaches 0.963 and 0.951, and the predicted displacements agree well with the observed displacements. By comparison, using the GA algorithm to optimize parameters can improve the accuracy of the SVM model better.

Although the proposed method yields relatively good results, if factors as the rainfall quantity or water level suddenly change, the error of point-based displacement prediction will inevitably increase. Thus, solving this problem becomes highly necessary. Therefore, in order to establish a more accurate causal relationship, the latest monitoring data should gradually be substituted, while the earlier information should be removed (Du et al. 2013).

Table 5 Optimal parameters and accuracy of the model

Point	C	g	R^2	RMSE
ZG118	1.19	49.74	0.771	5.799
XD-01	1.59	38.37	0.740	9.741

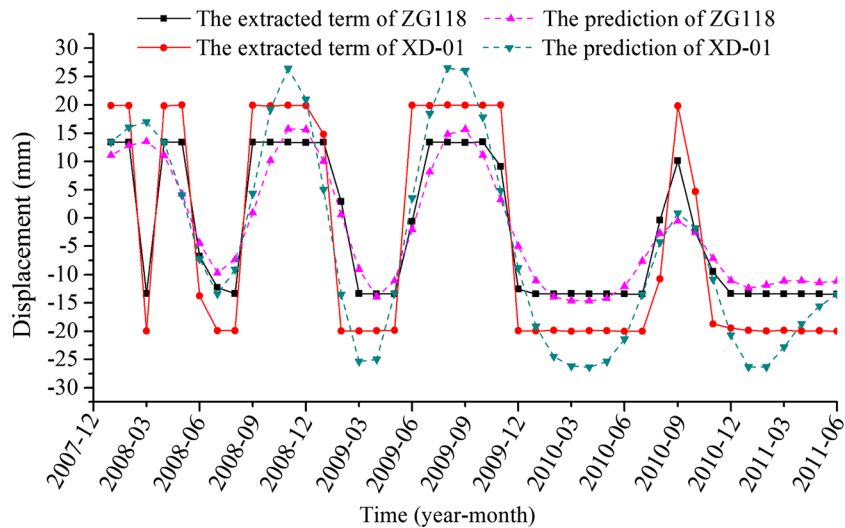


Fig. 17 Prediction and comparison of random displacement

Conclusions

The following conclusions were drawn from this study:

- (1) The general trend of deformation evolution is affected by internal factors. External factors, such as seasonal rainfall and reservoir water level fluctuations, directly accelerate the deformation and failure processes of the landslide. The external factors are the main reasons for the developmental of the “step-like” landslide in the Three Gorges Reservoir area. Therefore, the relationships between internal and external factors are important when analyzing the deformation mechanisms of a landslide.
- (2) The results of the periodic displacement calculations show that the prediction accuracy of the displacement prediction model based on GA-SVR is better than the prediction accuracy of other models based on GS-SVR and PSO-SVM. Therefore, the GA-SVR model has broad application potential for random displacement predictions.
- (3) The displacement sequence of a landslide can be divided into trend, periodic, and random terms, each with clear mathematical and physical significance. This approach was proven effective in this study. The method yields relatively good results for displacement prediction by coupling the GA-SVR model and time series data. However, abrupt changes in the rainfall quantity or water level will inevitably increase the error of point-based displacement prediction.

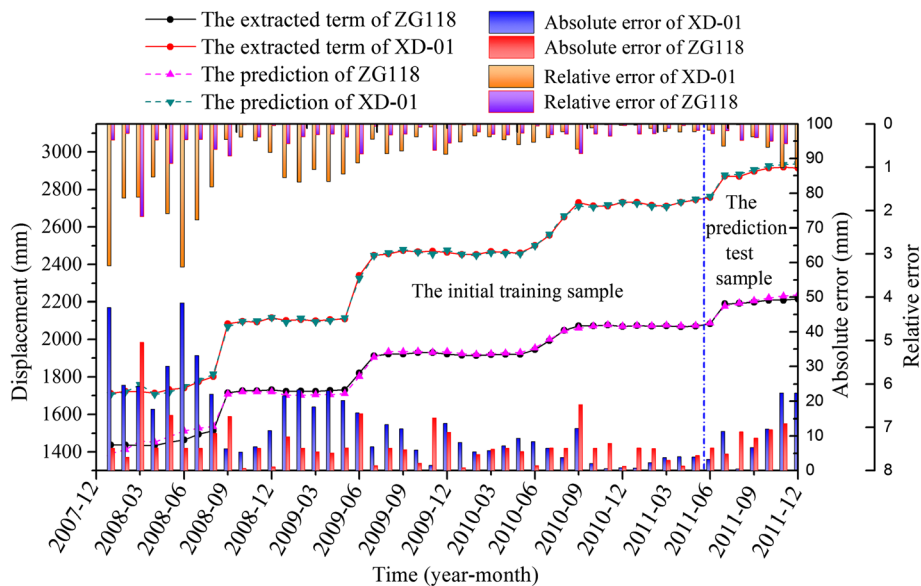


Fig. 18 The curves of the relationship between observed and predicted displacement

Acknowledgements

This research is supported by the National Natural Science Foundation of China (No. 41272307 and No. 41572278). We thank the colleagues in our laboratory for their constructive comments and assistance.

References

- Bernardie S, Desramaut N, Malet JP et al (2015) Prediction of changes in landslide rates induced by rainfall. *Landslides* 12(3):481–494
- Bordoni M et al (2015) Hydrological factors affecting rainfall-induced shallow landslides: from the field monitoring to a simplified slope stability analysis. *Eng Geol* 193:19–37
- Bui DT, Tuan TA, Klempe H et al (2016b) Spatial prediction models for shallow landslide hazards: a comparative assessment of the efficacy of support vector machines, artificial neural networks, kernel logistic regression, and logistic model tree. *Landslides* 13(2):361–378
- Bui DT, Tuan TA, Hoang ND, et al. (2016a) Spatial prediction of rainfall-induced landslides for the Lao Cai area (Vietnam) using a hybrid intelligent approach of least squares support vector machines inference model and artificial bee colony optimization. *Landslides* 1–12
- Bui DT, Tuan TA, Klempe H et al (2016c) Spatial prediction models for shallow landslide hazards: a comparative assessment of the efficacy of support vector machines, artificial neural networks, kernel logistic regression, and logistic model tree. *Landslides* 13(2):361–378
- Carlà T, Intrieri E, Traglia FD et al (2016) A statistical-based approach for determining the intensity of unrest phases at Stromboli volcano (Southern Italy) using one-step-ahead forecasts of displacement time series. *Nat Hazards* 84(1):669–683
- Carlà T, Intrieri E, Farina P et al (2017) A new method to identify impending failure in rock slopes. *Int J Rock Mech Mining Sci* 93:76–81
- Cao Y, Yin K, Alexander DE et al (2015) Using an extreme learning machine to predict the displacement of step-like landslides in relation to controlling factors. *Landslides* 13(4):725–736
- Chousianitis K, Gaudio V, Kalogeris I et al (2014) Predictive model of Arias intensity and Newmark displacement for regional scale evaluation of earthquake-induced landslide hazard in Greece. *Soil Dyn Earthq Eng* 65:11–19
- Crosta GB, Agliardi F (2003) Failure forecast for large rock slides by surface displacement measure. *Can Geotech J* 40(1):176–191(16)
- Crosta GB, Agliardi F (2012) How to obtain alert velocity thresholds for large rockslides. *Phys Chem Earth* 27(36):1557–1565
- Deng J (1988) Grey forecasting and decision making. Huazhong University of Science and Technology Press, Wuhan, pp 86–128
- Du J, Yin K, Lacasse S (2013) Displacement prediction in colluvial landslides, Three Gorges Reservoir, China. *Landslides* 10(2):203–218
- Du W, Wang G (2016) A one-step Newmark displacement model for probabilistic seismic slope displacement hazard analysis. *Eng Geol* 205:12–23
- Eberhart R, Kennedy J (1995) A new optimizer using particle swarm theory. Proceedings of the Sixth International Symposium on Micro Machine and Human Science. Nagoya, Japan, IEEE, pp 39–43
- Faculty of civil and construction, Three Gorges University (2013) Emergency management survey report of the Baishuihe Landslide, subsequent geological disaster prevention and control of Zigui County project in the Three Gorges Reservoir area. Three Gorges University, Hubei province
- Federico A, Popescu M, Elia G et al (2012) Prediction of time to slope failure: a general framework. *Environ Earth Sci* 66(1):245–256
- Fukuzono T (1985) A new method for predicting the failure time of a slope. Proceedings of the 4th International Conference and Field Workshop on Landslides, Tokyo. University Press, Tokyo, pp 145–150
- Gao X, Hou J (2016) An improved SVM integrated GS-PCA fault diagnosis approach of Tennessee Eastman process. *Neurocomputing* 174:906–911
- Hayashi S, Komamura F, Park B (1988) On the forecast of time to failure of slope–time process of slope failure. *J Jpn Landslide Soc* 24(4):11–18
- Hong H, Pradhan B, Xu C et al (2015) Spatial prediction of landslide hazard at the Yihuang area (China) using two-class kernel logistic regression, alternating decision tree and support vector machines. *Catena* 133:266–281
- Hong H, Pourghasemi HR, Pourtaghi ZS (2016a) Landslide susceptibility assessment in Lianhua County (China): a comparison between a random forest data mining technique and bivariate and multivariate statistical models. *Geomorphology* 259:105–118
- Hong H, Pradhan B, Bui DT, et al. (2016b) Comparison of four kernel functions used in support vector machines for landslide susceptibility mapping: a case study at Suichuan area (China). *Natural Hazards & Risk*
- Hong H, Pradhan B, Jebur MN et al (2016c) Spatial prediction of landslide hazard at the Luxi area (China) using support vector machines. *Environ Earth Sci* 75(1):1–14
- Huang R, Xu Q (1997) Collaborative forecasting model of slope instability time. *Mt Res* 01:7–12
- Hwang G, Chen C (2013) A study of the Newmark sliding block displacement functions. *Bull Earthq Eng* 11:481–502
- Jebur MN, Pradhan B, Tehrany MS (2015) Manifestation of LiDAR-derived parameters in the spatial prediction of landslides using novel ensemble evidential belief functions and support vector machine models in GIS. *IEEE J Sel Top Appl Earth Obs Remote Sens* 8(2):674–690
- Jiao Y, Zhang H, Tang H et al (2014) Simulating the process of reservoir-impoundment-induced landslide using the extended DDA method. *Eng Geol* 182:37–48
- Li D, Yin K, Leo C (2010) Analysis of Baishuihe landslide influenced by the effects of reservoir water and rainfall. *Environ Earth Sci* 60(4):677–687
- Li X, Zhang N, Liao Q et al (2004) Analysis of groundwater dynamic field under the combined action of reservoir water level fluctuation and rainfall. *Chin J Rock Mech Eng* 21:3714–3720
- Lian C, Zeng Z, Yao W et al (2015) Multiple neural networks switched prediction for landslide displacement. *Eng Geol* 186:91–99
- Liu X, Liu G, Chen W et al (2003) Comprehensive analysis of the impact of rainfall on slope deformation and failure. *Chin J Rock Mech Eng* 52:2715–2718
- Liu Z, Shao J, Xu W et al (2014) Comparison on landslide nonlinear displacement analysis and prediction with computational intelligence approaches. *Landslides* 11:889–896
- Mufundirwa A, Fujii Y, Kodama J (2010) A new practical method for prediction of geomechanical failure time. *Int J Rock Mech Min Sci* 47(7):1079–1090
- Newcomen W, Dick G (2016) An update to the strain-based approach to pit wall failure prediction, and a justification for slope monitoring. *J South Afr Inst Min Metall* 116(5):379–385
- Pradhan B (2013) A comparative study on the predictive ability of the decision tree, support vector machine and neuro-fuzzy models in landslide susceptibility mapping using GIS. *Comput Geosci* 51:350–365
- Qin S (2005) Nonlinear evolution mechanism and physical prediction of slope instability process. *Chin J Rock Mech Eng* 11:6–13
- Saito M (1965) Forecasting the time of occurrence of a slope failure. In: Proceedings of the 6th International Mechanics and Foundation Engineering, Montr, al, Que. Pergamon Press, Oxford 537–541
- Segoni S, Lagomarsino D, Fanti R et al (2015) Integration of rainfall thresholds and susceptibility maps in the Emilia Romagna (Italy) regional-scale landslide warning system. *Landslides* 12(4):773–785
- Taskin K, Emrehan KS, Ismail C (2015) Selecting optimal conditioning factors in shallow translational landslide susceptibility mapping using genetic algorithm. *Eng Geol* 192:101–112
- Tomas R, Li Z, Liu P (2014) Spatiotemporal characteristics of the Huangtupo landslide in the Three Gorges region (China) constrained by radar interferometry. *Geophys J Int* 197(1):213–232
- Vapnik V (2000) The nature of statistical learning theory. Springer-Verlag, New York USA, pp 138–167
- Voight B (1989) A relation to describe rate-dependent material failure. *Science* 243:200–203
- Wang Y, Yin K, An G (2004) Grey correlation analysis of landslide sensitive factor. *Rock Soil Mech* 01:91–93
- Yang S (1992) Engineering application of time series analysis. Huazhong University of Science and Technology Press, Wuhan
- Yao W, Zeng Z, Lian C et al (2015) Training enhanced reservoir computing predictor for landslide displacement. *Eng Geol* 188:101–109
- Yin K, Yan T (1996) Landslide prediction and related models. *Chin J Rock Mech Eng* 01:1–8
- Zhou C, Yin K, Cao Y et al (2016) Application of time series analysis and PSO–SVM model in predicting the Bazimen landslide in the Three Gorges Reservoir, China. *Eng Geol* 204:108–120

F. Miao · Y. Wu · Y. Xie · Y. Li

Engineering Faculty,
China University of Geosciences,
Wuhan, 430074, China

Y. Wu (✉)

Three Gorges Research Center for Geo-hazard,
Wuhan, 430074, China
e-mail: wyp892@126.com